Particle Accelerators, Vol. 59, pp. 143–156
Reprints available directly from the publisher
Photocopying permitted by license only

A RIPPLE EFFECT OF A KLYSTRON POWER SUPPLY ON SYNCHROTRON OSCILLATION

M. HARA*, T. NAKAMURA and T. OHSHIMA

SPring-8, JASRI, Kamigori, Ako-gun, Hyogo-ken 678-12, Japan

(Received 6 August 1997; In final form 17 November 1997)

Coherent synchrotron oscillation was observed in the SPring-8 storage ring as sidebands at the harmonics of the accelerating frequency, which is independent of beam current. This is explained using a forced oscillation model of the synchrotron oscillation affected by the disturbance of accelerating voltage. The RF disturbance is induced by the ripple noise in the klystron power supply at the harmonics of the frequency of the AC power supply.

Keywords: Ripple; Coherent synchrotron oscillation; Forced oscillation; RF phase noise

1 INTRODUCTION

High voltage DC power supplies are an integral part of most particle accelerators. However, they tend to produce ripple noise that detracts from the accelerator's overall performance. If a klystron power supply has excessive ripple noise, electron beams accelerated by a cathode voltage in the klystron suffer from ripple effects that modulate their velocities, and, as a consequence, amplified RF is modulated. If one of the frequency components is close to the synchrotron oscillation frequency, the ripple noise induces a coherent synchrotron oscillation.

* Corresponding author. Tel.: 81-7915-8-0863. Fax: 81-7915-8-0850.
E-mail: hara@sp8sun.spring8.or.jp.

The ripple noise effects in the SPring-8 storage ring were measured by varying the effective accelerating voltage. These effects were found to be a sideband signal of the accelerating frequency (508.58 MHz); and the sideband signal frequency was a higher harmonic of the AC power supply (i.e., integral multiples of 360 Hz).

Experimental evidence indicates that the design of a low-level RF system should pay special attention to the relationship between the ripple frequency of the klystron power supply and the synchrotron oscillation frequency.[1] The effect of RF phase noises on the electron beam were recently investigated theoretically.[2] In the SPring-8 storage ring, coherent synchrotron oscillation caused by high voltage ripples in the klystron was found to be a sideband peak of the acceleration frequency; and the strength of the sideband can be explained by a simple forced oscillation model.

2 KLYSTRON PHASE DELAY

A schematic diagram of a klystron is shown in Figure 1. Electrons are emitted from a cathode and accelerated by a cathode–collector voltage and captured by a collector that is usually connected to the earth. Input, output, and other cavities are installed between the anode and collector. Electrons are velocity-modulated by the input cavity, which is excited at RF frequency, and pass through drift space. On the way to the collector, the electrons are bunched by velocity modulation; and the bunched electrons induce the RF voltage in the output cavity.

Slight changes in the cathode voltage affect the electron travel time T, causing a phase delay in the RF output voltage. The phase delay $\Delta\theta_D$ can be calculated from the following relations:

$$\theta_D = 2\pi f_{\mathrm{RF}} T, \tag{1}$$

$$T = \frac{L}{c\beta}, \tag{2}$$

$$\beta = \sqrt{1 - \frac{1}{\gamma^2}}, \tag{3}$$

$$\gamma = \frac{eV_{\mathrm{k}}}{mc^2} + 1, \tag{4}$$

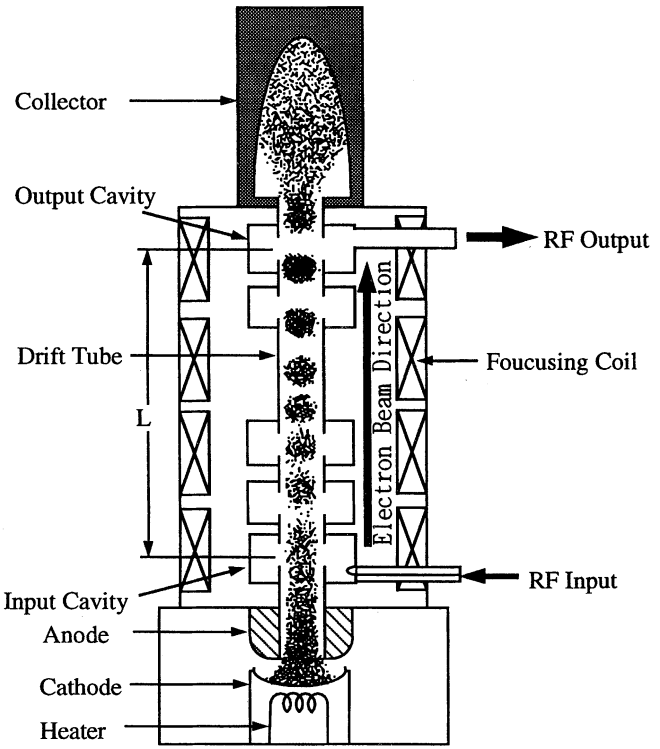

FIGURE 1 Schematic diagram of a klystron.

where: f_{RF} is the RF frequency; L the length between the input cavity and the output cavity; β the dimensionless velocity of the electron beam; c the velocity of light; γ the dimensionless energy of the electron beam; $-V_k$ the cathode voltage; e electron charge; and mc^2 the electron rest mass energy.

Voltage fluctuation ($\Delta V_k/V_k$) coefficient D for the phase delay is calculated from Eq. (1),

$$D \equiv V_k \frac{d\theta_D}{dV_k} = -2\pi f_{RF} \frac{L}{c} \frac{1}{(\beta\gamma)^3} \frac{eV_k}{mc^2}. \tag{5}$$

This can be rewritten as

$$\Delta\theta_D = D \frac{\Delta V_k}{V_k}. \tag{6}$$

To get the physical image, the coefficient D is estimated numerically and shown in Figure 2, where $L = 2.5$ m, and $f_{RF} = 508.58$ MHz. If the klystron is operated at a cathode voltage of 80 kV, a ripple noise of $\Delta V/V = 10^{-3}$ induces a phase difference of 1.2°. This is comparable to the bunch length $\sigma_\theta = 2.44°$ in the SPring-8 storage ring.

The phase delay induces a phase modulation in the RF frequency in an acceleration cavity. If the cathode voltage of the klystron has a ripple component of $\Delta V_k \sin \omega t$, the output signal of the klystron $A \sin(\omega_{RF} t + \phi)$ is phase-modulated and can be expressed as

$$
\begin{aligned}
&A \sin\left(\omega_{RF} t + D \frac{\Delta V_k}{V_k} \sin \omega t\right) \\
&\quad = A \sin(\omega_{RF} t + a \sin \omega t) \\
&\quad = A(\sin \omega_{RF} t \cos(a \sin \omega t) + \cos \omega_{RF} t \sin(a \sin \omega t)) \\
&\quad = A \sin(\omega_{RF} t)\left(J_0(a) + 2 \sum_{n=1}^{\infty} J_{2n}(a) \cos 2n\omega t\right) \\
&\qquad + A \cos(\omega_{RF} t)\left(2 \sum_{n=1}^{\infty} J_{2n-1}(a) \sin((2n-1)\omega t)\right) \\
&\quad = A J_0(a) \sin \omega_{RF} t + A \sum_{n=1}^{\infty} J_{2n}(a)(\sin(\omega_{RF} + 2n\omega)t + \sin(\omega_{RF} - 2n\omega)t) \\
&\qquad + A \sum_{n=1}^{\infty} J_{2n-1}(a)(\sin(\omega_{RF} + (2n-1)\omega)t - \sin(\omega_{RF} - (2n-1)\omega)t),
\end{aligned}
\tag{7}
$$

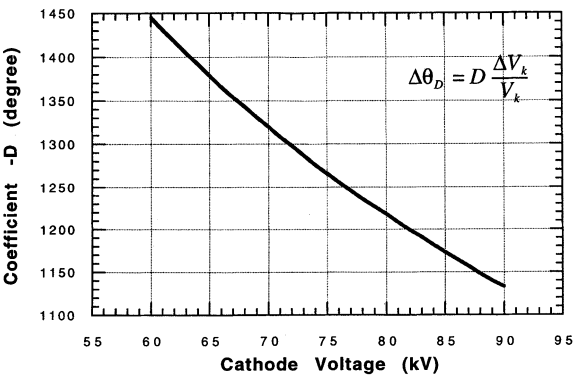

FIGURE 2 Coefficient D to estimate phase delay for a given $\Delta V/V$. In this graph, $-D$ is displayed because D is negative.

where $D\Delta V_k/V_k$ is replaced by a. From the equation, phase modulation effects appear as a sideband signals at $\omega_{RF} \pm \omega$ and the amplitude is

$$J_1\left(D\frac{\Delta V_k}{V_k}\right) = \frac{1}{2}D\frac{\Delta V_k}{V_k} \quad \text{for } D\frac{\Delta V_k}{V_k} \ll 1. \tag{8}$$

3 BUNCH RESPONSE

The equation for small phase oscillations τ in a bunch is given by[3]

$$\frac{d^2\tau}{dt^2} + 2\alpha_\epsilon\frac{d\tau}{dt} + \Omega^2\tau = 0, \tag{9}$$

where α_ϵ is damping coefficient given by

$$\alpha_\epsilon = \frac{1}{2T_0}\left(\frac{dU_{rad}}{dE}\right)_{E_0}, \tag{10}$$

U_{rad} is a radiation energy loss per turn of an electron with an energy E, and Ω is the synchrotron oscillation (angular) frequency given by

$$\Omega^2 = \frac{\alpha e\dot{V}_{RF}}{T_0E_0}, \tag{11}$$

where α, T_0, E_0, and V_{RF} are the momentum compaction factor, the revolution time, the electron energy, and the accelerating voltage, respectively. For a sinusoidal accelerating voltage,

$$V_{RF} = V_0\sin(\omega_{RF}t + \phi_s), \tag{12}$$

$$\Omega^2 = \frac{\alpha e\omega_{RF}V_0\cos\phi_s}{T_0E_0}, \tag{13}$$

where ω_{RF} and ϕ_s are the acceleration angular frequency and the synchronous phase.

The phase modulation or amplitude modulation affects Ω^2 through $\dot{V}_{RF}$. This modulation can be treated as an external force in a simple forced oscillation model.

$$\frac{d^2\tau}{dt^2} + 2\alpha_\epsilon\frac{d\tau}{dt} + \Omega^2\tau = \frac{\Omega^2}{\omega_{RF}}\Delta\theta_D e^{j\omega t}, \tag{14}$$

or

$$\frac{d^2\tau}{dt^2} + 2\alpha_\epsilon \frac{d\tau}{dt} + \Omega^2\tau = \frac{\Omega^2}{\omega_{RF}} \frac{\Delta V}{V} e^{j\omega t}. \tag{15}$$

Solution of Eq. (14) can be expressed as

$$\tau = \frac{(\Omega^2/\omega_{RF})\Delta\theta_D e^{j\omega t}}{\sqrt{(\Omega^2 - \omega^2)^2 + 4\alpha_\epsilon^2\Omega^2}}. \tag{16}$$

Equations (14) and (15) are equivalent and the solution of Eq. (15) can be expressed as Eq. (16) if $\Delta\theta_D$ is replaced with $\Delta V/V$.

A ripple of angular frequency ω in a klystron power supply induces synchrotron oscillation with amplitude expressed by Eq. (16). If the accelerating voltage is changed for a fixed ω, the amplitude is maximum at $\Omega = \omega$ and the width is given by α_ϵ. If there is more than one value for ω and the coherent synchrotron oscillation is measured, the peak amplitude is larger for a smaller ω.

From Eqs. (14) and (15), the accelerating voltage modulation and phase modulation give the same results, and the mechanism is determined by the magnitude of $\Delta\theta_D$ and $\Delta V/V$. If $\Delta\theta_D$ is larger than $\Delta V/V$, the forced oscillation will be induced by phase modulation. The phase detector signal and klystron forward power were measured in the SPring-8 storage ring RF system and it was confirmed that $\Delta\theta_D$ was larger than $\Delta V/V$ as is shown in Figure 10 later.

4 SYNCHROTRON OSCILLATION AMPLITUDE

The quantitative amplitude from the measured synchrotron oscillation power spectrum can be obtained from the equations below. Cited from Ref. [4], a single particle longitudinal signal at time t and angular azimuth position θ can be described as

$$s_\parallel(t, \theta) = e \sum_{n=-\infty}^{\infty} \delta\left(t - \tau - \frac{\theta}{\omega_0} - \frac{2n\pi}{\omega_0}\right), \tag{17}$$

where: δ is the Dirac function; τ the time interval between the reference particle passing and test particle passing; and ω_0 the angular

revolution frequency. Fourier transform of Eq. (17) gives a line spectrum at frequencies $\omega_{pm} = p\omega_0 + m\omega_s$:

$$\tilde{s}_{\parallel}(\omega, \theta) = \frac{e\omega_0}{2\pi} \sum_{p,m=-\infty}^{\infty} j^{-m} J_m(p\omega_0\hat{\tau}) e^{j(p\theta - m\psi_0)} \delta(\omega - \omega_{pm}), \tag{18}$$

where $J_m(x)$ is a Bessel function; $\hat{\tau}$ the synchrotron oscillation amplitude; and ω_s the synchrotron oscillation angular frequency. The spectrum amplitude at the revolution frequency and the first sideband are described as

$$S_{0s}(p) = IJ_0(p\omega_0\hat{\tau}), \tag{19}$$

$$S_{1s}(p) = IJ_1(p\omega_0\hat{\tau}), \tag{20}$$

where I is the electron current and p is an integer. Power spectrum is the square of the amplitude, and the power spectrum ratio is given as

$$R_s(p) = \left(\frac{S_{1s}(p)}{S_{0s}(p)}\right)^2 = \left(\frac{J_1(p\omega_0\hat{\tau})}{J_0(p\omega_0\hat{\tau})}\right)^2. \tag{21}$$

Above is the single particle model, which is illustrated in Figure 3. Using this model, excited synchrotron oscillation amplitude can be estimated.

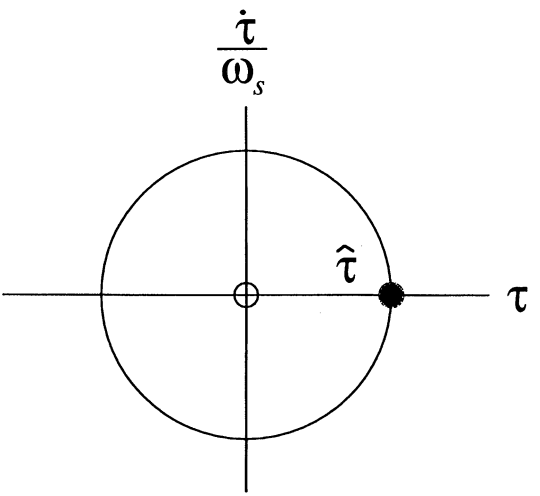

FIGURE 3 Synchrotron oscillation in single particle model.

5 MEASUREMENT

The SPring-8 storage ring has four RF stations. Each station has 8 single-cell cavities which are powered by 1 MW klystron. At the commissioning stage three RF stations (B, C, and D) are installed. The specification of the klystron and power supply is listed in Table I.

The power supply is thyristor regulated and has no crowbar circuit and no large capacitor bank.[5] Each power supply is basically a six-phase rectifier circuit (with ripple noises occurring in integral multiples of 360 Hz): and the klystron power supplies in the three stations are phase shifted by 20° from each other at their input transformer. Therefore, if each station is finely tuned and three stations are balanced, equivalent 18-phase rectifier could be expected (with ripple noises in integral multiples of 1080 Hz). In fact, there are some causes that disturb the balances, so that the extra harmonic components are excited in the power supply. An example of the ripple measurements of the power supply using an FFT analyzer is shown in Figure 4.

TABLE I Specification of klystron and power supply

Klystron	E3786 (Toshiba)
Frequency	508.58 MHz
Output power	1 MW (CW)
Power supply	Thyristor regulated with six phase
Maximum voltage	−90 kV
Maximum currents	20 A
AC power line frequency	60 Hz
Voltage ripple	0.5% p–p (at 360 Hz)

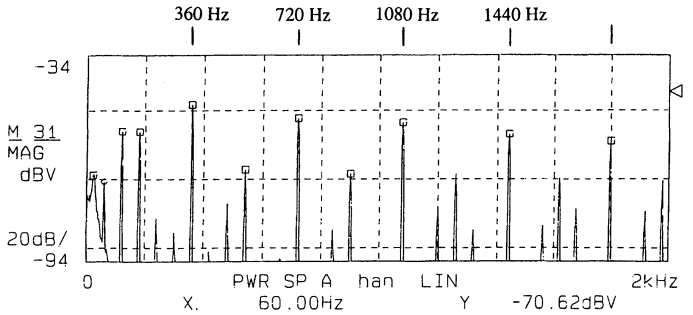

FIGURE 4 An example of the power supply ripple noise spectrum below 2 kHz for D station. $V_{\text{cathode}} = 60$ kV. Measured by CF-360 portable dual channel FFT analyzer.

In this case, frequency components in integral multiples of 360 Hz can be seen at the level $\Delta V/V \approx 10^{-3}$. Frequency components of 60, 180, 540 Hz, etc., were also observed in the power supply output, which comes from the above stated unbalance. Low frequency components of less than 1 kHz can be reduced by automatic level control (ALC) and phase lock loop (PLL) in the low power RF system. These are referred later.

Sideband of coherent synchrotron oscillation is proportional to $J_1(p\omega_0\hat{\tau})$, therefore, it is necessary to measure at an appropriate frequency to observe the synchrotron oscillation (not too low $p\omega_0\hat{\tau}$). The electron beam signal from a Beam Position Monitor (BPM) was measured at the acceleration frequency (508.58 MHz, $p=2436$). Cavity voltages (measured by the pickups attached to the cavities and vector summed) at three stations (B, C, and D) were kept constant (set voltages were $V_b=$ 5.13 MV, $V_c=4.89$ MV and $V_d=3.54$ MV after calibration), and the phase of the B station (θ_b) was varied (Figure 5). Stored currents were about 200 μA.

The power spectrum was measured using spectrum analyzer (HP8591E) and an example of the raw data is shown in Figure 6. We can see the sideband peaks of the coherent synchrotron oscillation around the acceleration frequency. These peaks do not originate in collective phenomena because the current is very low. Sideband peak frequencies are plotted for θ_b in Figure 7.

Observed sideband peak frequencies were confined to the integral multiples of 360 Hz ($n \times 360$, $n=3, 4, 5$) near the synchrotron oscillation frequency. The solid line in the figure represents the calculated synchrotron oscillation frequencies at θ_b, assuming a designed momentum compaction factor of $\alpha = 1.46 \times 10^{-4}$.

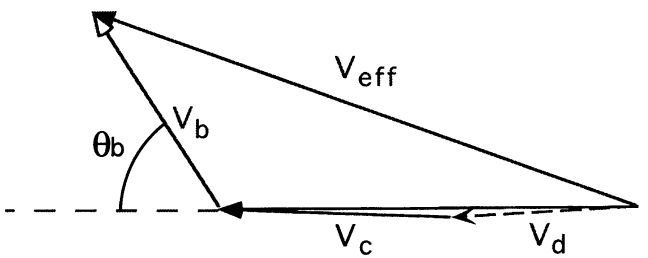

FIGURE 5 Voltage and phase relation of B, C, D stations and the effective voltage.

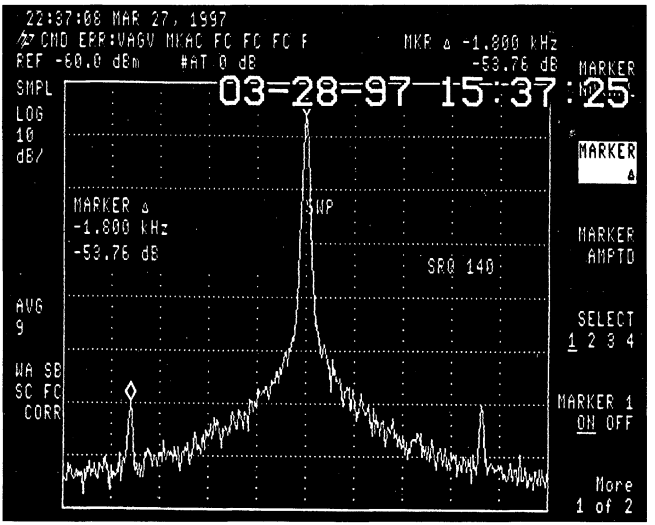

FIGURE 6 An example of spectrum data taken at $\theta_b = 18°$. The large peak in the center is the accelerating frequency 508.589362 MHz; and the sideband peaks are observed clearly at integral multiple of 360 Hz (1800 Hz). Synchrotron oscillation frequency calculated from the design value of momentum compaction factor is 1732 Hz.

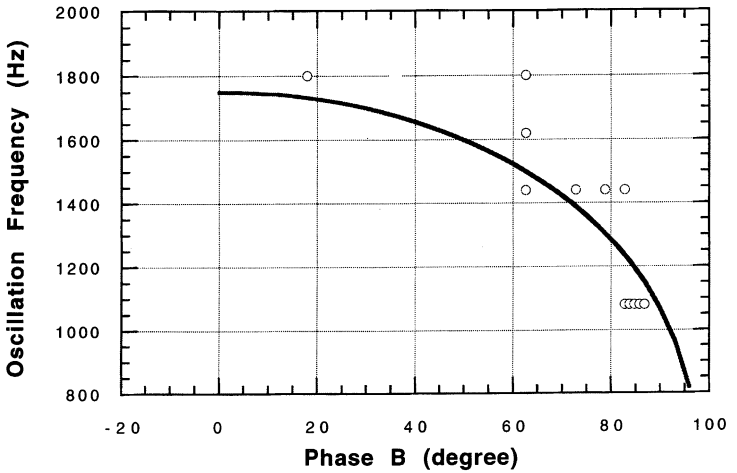

FIGURE 7 Frequencies of the sideband are plotted as a function of θ_b. Circles indicate the observed peak frequencies and the line is the calculated synchrotron oscillation frequency. Observed peaks are on the integral multiples of 360 Hz. A peak at 1620 Hz (180×9) is also seen.

The intensity of the sideband signals at 1080, 1440, and 1880 Hz, divided by that of the accelerating frequency, are plotted at the corresponding synchrotron oscillation frequencies in Figure 8. The peak power spectrum values on the accelerating frequency are proportional to the stored current. Therefore, the ratio of sideband intensity to the accelerating frequency is equal to the current normalized intensity of the sideband signal. It is the ratio, not the sideband signal itself, that determines the physical quantity. Sideband signals at 1080 Hz peak at $f_s = 1150$ Hz or less, while at 1440 Hz they peak at $f_s = 1400$ Hz, and that at 1800 Hz have a rising shoulder around 1700 Hz. The lines in the figure are calculated from the forced oscillation model. Chain, dotted, and solid lines are calculated using ω in Eq. (16) set to $2\pi \times 1080$, $2\pi \times 1440$, and $2\pi \times 1800$, respectively. This model reproduces these sideband amplitude fairly well.

Figure 8 shows that maximum intensity ratio is measured to be about 10^{-4} at 1080 Hz sideband. The single particle model in Section 3 provides a basis for estimating the forced synchrotron oscillation amplitude: Ratio based on the single particle model is expressed by Eq. (21); the calculated coherent synchrotron oscillation amplitude in length is shown as a function of power spectrum ratio in Figure 9. From this calculation, maximum forced coherent synchrotron oscillation

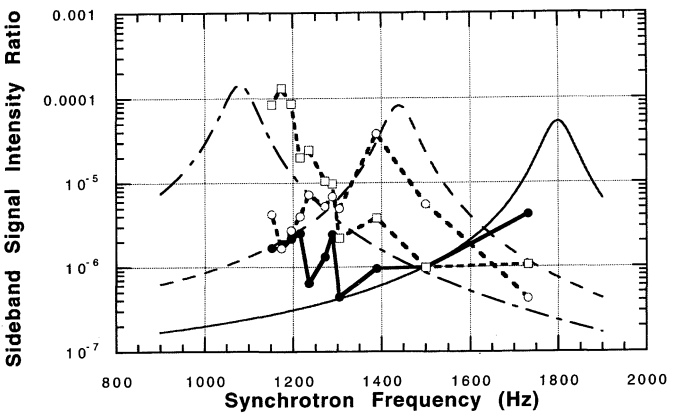

FIGURE 8 Sideband signal intensities at 1080, 1440, and 1800 Hz divided by the accelerating frequency signal of 508.58 MHz. The squares, circles and solid circles represent data at 1080, 1440, and 1800 Hz, respectively. Three curves are calculated using the forced oscillation model Eq. (16).

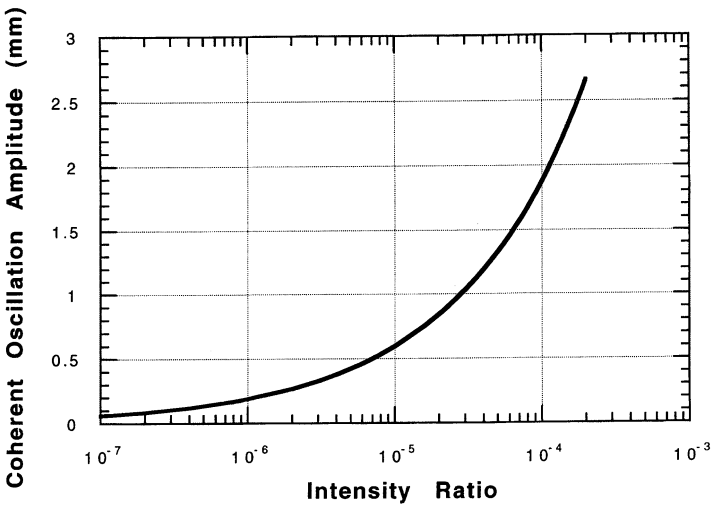

FIGURE 9 Coherent synchrotron oscillation amplitude based on a single particle model.

amplitude is 1.5–2 mm while the nominal bunch length is estimated to be about 4 mm.

6 DISCUSSION

The performance of the RF low power system of the storage ring was measured,[6] which is equipped with an automatic level control (ALC) and phase lock loop (PLL). The klystron forward phase and RF voltage with ALC and PLL -off and -on in B station are shown in Figures 10(a) and (b). From the figures, you can see the amplitude fluctuation $\Delta V/V$ was 1.5×10^{-2} and 3.7×10^{-3} with ALC -off and -on while the phase fluctuation $\Delta\theta_D$ was 3° and 1.4° with PLL -off and -on. As klystron power supply is based on thyristor control, the corresponding ripple extends to several kHz. The feedback loops are effective below 1 kHz but not above 1 kHz, where sharp spikes remain even with ALC and PLL -on. In order to reduce the ripple effects, it is necessary to fine tune each power supply and balance the three stations; and improve the feedback system so that it can adapt to a wider frequency range.

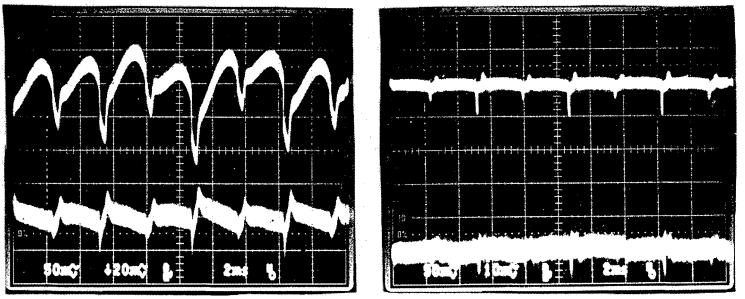

(a) (b)

FIGURE 10 Raw data of phase and forward output voltage of the klystron with ALC -off (a) and -on (b). The upper is the output signal of phase detector and the bottom is that of RF linear detector. The axis of abscissas is 50 ms/div, and that of the ordinate is 50 mV/div. The scale of the phase is 1°/50 mV and the DC level of the output voltage is 2.7 V for both (a) and (b).

Sideband signals from the accelerating frequency were measured at low current by varying the effective cavity voltage by means of a station phase. The measured sideband frequencies were integral multiples of 360 Hz. The characteristics of the signal are fairly well explained by a simple forced oscillation model. Though the peak position of the sideband signal is a little bit different from the calculated one, this comes from the errors in calibrating cavity voltage, phase, momentum compaction factor and so on. The origin of the forced oscillation is the phase modulation rather than amplitude modulation, because the amplitude fluctuation $\Delta V/V$ of 1.5×10^{-2} and 3.7×10^{-3} is equivalent to the phase fluctuation $\Delta\theta_D$ of 0.85° and 0.2°, which is much smaller than the phase modulation itself.

7 CONCLUSION

Coherent synchrotron oscillation is excited by the klystron phase noise that comes from a ripple. The observed signal frequencies are in integral multiples of 360 Hz near synchrotron oscillation frequency. The excitation of coherent synchrotron oscillation is caused by power supply ripples through forced oscillation of a phase modulation mechanism. The induced coherent oscillation amplitude is about 2 mm in length, while the nominal bunch length due to the

synchrotron oscillation is about $\sigma_l = 4\,\text{mm}$. In order to reduce this ripple effect, it is useful to balance the power supplies of the three stations and to improve the phase feedback system.

Acknowledgements

The authors wish to thank the members of the commissioning and operation group of SPring-8 for the data taking, Dr. Y. Miyahara for his helpful discussion and preparation for the manuscript, and the member of RF group for useful discussion.

References

[1] E. Ezura, K. Arai, H. Hayano, M. Ono, M. Suetake and T. Takashima, *Proc. 1987 IEEE PAC*, 1660 (1987).
[2] Schin Daté, Kouichi Soutome and Ainosuke Ando, *NIM A* **355** (1995) 199–207.
[3] Mathew Sands, The Physics of Electron Storage Rings an Introduction.
[4] J.L. Laclare, Bunched beam coherent instabilities, CERN 87-03, 21 April 1987.
[5] N. Kumagai, C. Yamazaki and H. Kouzu, Star-point control for the klystron power supply in the SPring-8 storage ring, *Proc. Int. Power Electronics Conf.*, Yokohama, p. 1497 (1995).
[6] Y. Ohashi, H. Ego, M. Hara, N. Hosoda, Y. Kawashima, T. Ohshima, H. Suzuki, T. Takashima and H. Yonehara, SPring-8 Annual Report, 161 (1996).